

# New floating floor design with optimum isolator location

C.K. Hui\*, C.F. Ng

*Department of Civil and Structural Engineering, The Hong Kong Polytechnic University, Hung Hom, Hong Kong*

Received 15 May 2006; received in revised form 15 January 2007; accepted 15 January 2007  
Available online 6 March 2007

---

## Abstract

In this paper, a new design concept of an isolated honeycomb floor with a special arrangement of isolators is proposed to improve the vibration isolation performance of conventional lightweight cement floor panels in the frequency range of 120–600 Hz. The symmetric bending resonance frequencies and mode shapes of a honeycomb floor panel were identified by a shaker test. The effects on vibration isolation of isolator position and acoustic insulation were then investigated using experimental modal analysis. The analysis suggests that four design features ensure the optimum vibration isolation performance of a square floating honeycomb floor: the floor panel should be small, stiff, and lightweight; the isolators must be placed at the nodal points of the symmetric bending modes of the floor panel; the vibration must be transmitted via the center point of the floor panel; and acoustic insulation material should be installed inside the cavity. The proposed floating floor design achieved a vibration reduction of 20–30 dB in the frequency range of 120–600 Hz. In addition, the proposed floor was found to have a 20 dB lower vibration level at the first bending resonance frequency than the conventional design with isolators that are placed at the edges.

© 2007 Elsevier Ltd. All rights reserved.

---

## 1. Introduction

The isolation design was originally used in machine vibration control, but is now applied to floating floors that are used in ships, trains, airplanes, and buildings to enhance human comfort and decrease damage to equipment.

The size of conventional floating floor panels is usually rather large (about  $1 \times 2$  m) for production and installation convenience. Experimental investigations on these large floor panels have been conducted by various authors [1–3]. However, Kawaharazuka et al. [4] concluded that the vibration isolation efficiency of floating slabs is degraded by the low bending resonance frequencies that are induced in floor panels of this size. It is therefore logical that floating floor panels should be made smaller to increase their bending resonance frequencies.

Floating floor panels are usually made of concrete, wood, or steel. Heavy concrete slabs have generally lower acoustic transmission levels than lightweight floor panels at high frequencies [5], but are not commonly used due to their heavy weight. Thinner cement panels that are 15–40 mm thick are used, but their vibration isolation performance is still unsatisfactory. Honeycomb floor panels have a greater stiffness to mass ratio,

---

\*Corresponding author. Tel.: +852 2766 4480; fax: +852 2334 6389.  
E-mail address: [05900377r@polyu.edu.hk](mailto:05900377r@polyu.edu.hk) (C.K. Hui).

and are used extensively in aircraft for vibration reduction and sound insulation [6,7]. To enhance the vibration isolation performance of typical lightweight cement floor panels, small honeycomb panels with a high stiffness to damping ratio should be employed.

Most research in this area has focused on the identification of the best combination of material parameters in floating floor systems to enhance the vibration isolation performance at the receiver. Jutulstad [8] created a model to identify the best combination of the bending stiffness of plates and the distance between isolators. Baron [9] investigated the effects of different parameters of floating floors, including stiffness, dimension, and mass, on their isolation efficiency performance. Mead [10] suggested the method of nodalization to reduce the vibration input from a source by placing the source at the nodal points of a beam. Yan and Xie [11] analyzed the effect of positioning isolators at the base of electronic equipment to achieve rigid body vibration attenuation. However, there no theoretical model or experimental study has developed the concept of arranging the isolators at the nodal points of a plate to attenuate the bending mode vibration.

From previous test results, it can be established that very few floating floor types can provide a vibration isolation of 30 dB in the frequency range of 120–600 Hz. Some typical levels of vibration reduction for various material are 10 dB at 250 Hz and 15 dB at 500 Hz for honeycomb floor panel systems that are designed for aircraft [1], 15 dB at 250 Hz and 20 dB at 500 Hz for metal floor panels that are used in ships [2], and 15 dB at 250 Hz and 25dB at 500 Hz for cement floor panels that are used in dwellings [12]. The main reasons for the poor vibration isolation performance of typical floating floor designs are the large size of the floor panels and the placement of the isolators at the edge of the panel.

In this paper, experimental modal analysis is conducted to examine the method of increasing the vibration isolation performance of typical lightweight cement panels by the addition of a honeycomb floor panel with a high stiffness to mass ratio. An isolator position design is proposed to reduce the bending mode resonance of floor panels, which is the main cause of poor vibration isolation performance (the typical range is 120–600 Hz).

The remainder of this paper is organized as follows. Section 2 evaluates the dynamic properties of square honeycomb and cement panels with free boundary conditions through center excitation using a shaker, and identifies the common nodal point of the lowest symmetric bending modes of the two panel types. Section 3 introduces the theory of the effect of isolator position on transmissibility. Sections 4–6 report an analysis of the vibration reduction performance of different floor panels using an impact test. The air-borne and structure-borne energy transmission from the base structure to the floor panel receiver are analyzed separately with different measurement techniques to identify the optimum device for installation in floating floors. In Section 7, the vibration isolation performance of the proposed design is compared to some conventional floating floor designs. In the final section, the application of the proposed design is discussed.

## 2. Mode shape measurement and nodal line identification

### 2.1. Experimental setup

The experimental setup that is shown in Fig. 1 aims to find the resonance response and mode shape of cement and honeycomb panels and to identify the nodal points. The dimensions and material properties of the honeycomb panel (including the core design) and the cement panel that are studied are given in Table 1. Soft rubber was placed between the center of the panels and the vibrating shaker head. The boundary conditions were assumed to be free along the circumference of the plate. A white noise signal was used to drive the shaker to generate a wide band frequency (0–1.6 kHz) force, and an accelerometer was mounted on the shaker head to register the input acceleration to the panels. A lightweight accelerometer was mounted at various points on the panels to measure their acceleration response. The two acceleration signals were fed into the analyzer and a computer for data processing. Table 2 lists the instruments used. The analyzer worked in real time at the frequency resolution of 6400 lines in the range of 0 Hz–1.6 kHz. The frequency response functions (FRFs; the acceleration on the panel/shaker head), which are also known as the motion transmissibility, were obtained.

For the mode shape measurement, the center excitation acceleration with response acceleration along the surfaces of the panels was measured. The value of the imaginary part of the FRFs for a given resonance was assumed to be proportional to the modal displacement, and thus the mode shapes were established.

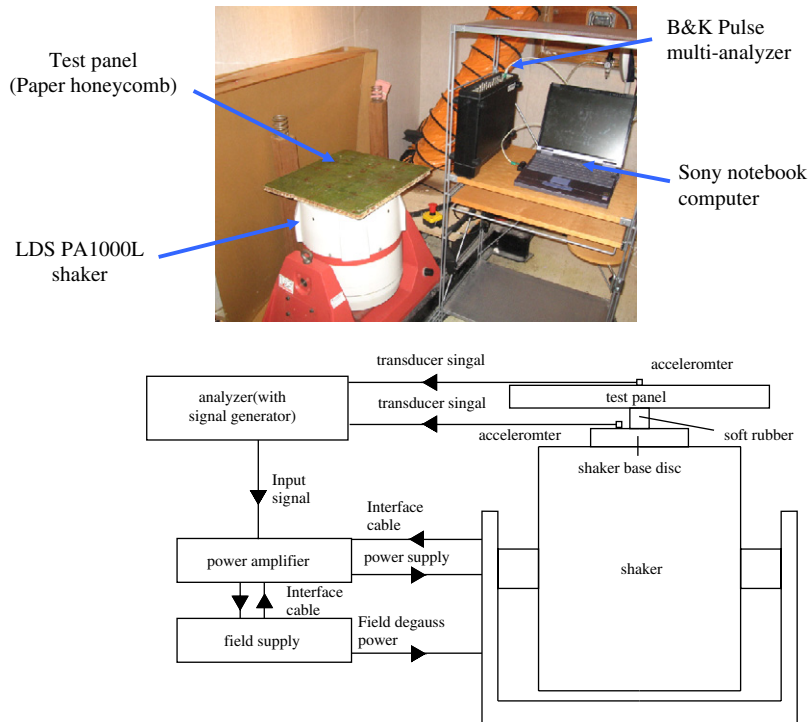


Fig. 1. Experimental setup of the mode shapes and resonance frequencies measurement.

Table 1  
Dimensions and material properties of the testing material

| Material        | Description  | Panel size (mm)<br>(length × width × height) | Young's modulus ( $E$ )<br>( $\times 10^9 \text{ N/m}^2$ ) | Density ( $\rho$ )  |
|-----------------|--|--|--|---|
| Paper honeycomb | Sandwich structure with Nomex paper core and covered with two glass reinforced plastics surface sheets (0.5 mm thickness for each surface sheet) | 415 × 415 × 15                               | Overall = 3.0<br>Surface sheet = 4.0<br>Core shear = 0.9   | Overall = 5.8 kg/m <sup>2</sup><br>Surface Sheet = 2550 kg/m <sup>3</sup><br>Core = 244 kg/m <sup>3</sup> |
| Cement          | Wood fibre chemically treated and mixed with Portland cement, compressed and cured under temperature controlled conditions                       | 520 × 520 × 15                               | 6.8  | 21.4 kg/m <sup>2</sup>  |

Table 2  
List of instruments used for experimental studies

| Item                      | Manufacturer | Model no.                 |
|---------------------------|--------------|---------------------------|
| Accelerometer             | ENDEVCO      | 752A12                    |
| Accelerometer             | B&K          | 4518–003 (light-weighted) |
| Microphone + preamplifier | B&K          | 4167 + 2671               |
| Shaker                    | LDS          | PA1000L                   |
| Analyzer                  | B&K (PULSE)  | Multi-analyzer 3560c      |

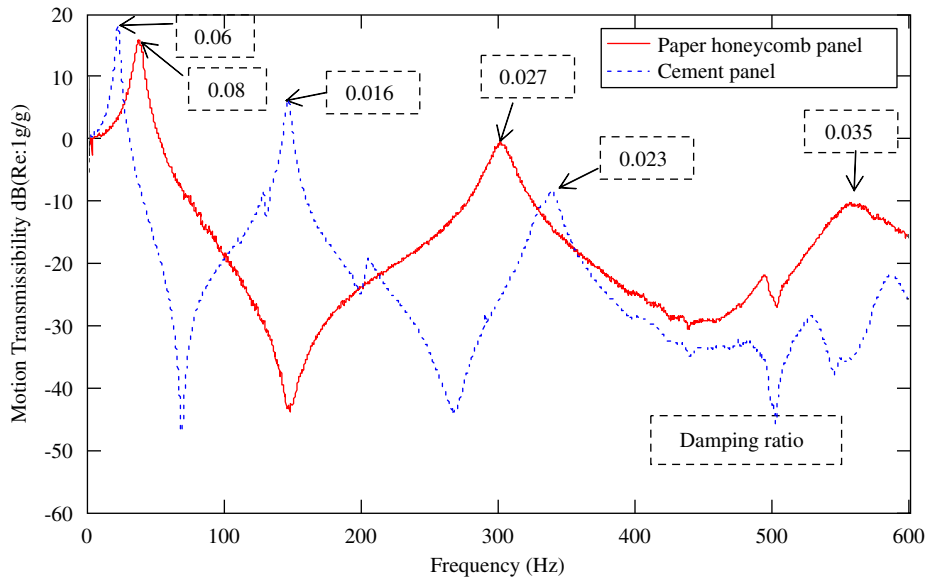


Fig. 2. Motion transmissibility (magnitude) and damping ratio of paper honeycomb panel and cement panel.

## 2.2. Experimental results

The motion transmissibility at the center point of the cement panel and the honeycomb panel is shown in Fig. 2. The damping ratio of each mode, which was identified using the half-power point method, is also given in Fig. 2. The resonance frequencies are 37.25, 300.5, and 556 Hz for the honeycomb panel, and 21.5, 145.5, and 337.5 Hz for the cement panel. The lowest resonance frequency is the rigid body mode, and the others are the bending modes. The negative value of the motion transmissibility implies that there was some vibration reduction from the vibration source to the receiver on the panel. The first bending resonance frequency of the honeycomb panel is much higher than that of the cement panel due to the higher stiffness to mass ratio. It can also be observed in Fig. 2 that there is a weak point of vibration isolation on the conventional cement panel at the first bending resonance frequency of 145.5 Hz. Fortunately, the honeycomb panel has an anti-resonance dip, and thus reduces the first bending mode of the cement panel at 145.5 Hz if it is added to the cement panel as a type of floating floor. However, the cement panel still has an additional resonance at 337.5 Hz that is close to that of 300.5 Hz of the honeycomb panel. This problem must be tackled by the suitable positioning of the isolators to isolate the vibration resonance near 300 Hz.

The identified mode shapes of the honeycomb panel at 300.5 and 556 Hz are shown in Fig. 3. In the contour plot graphs, the solid lines and the dashed lines represent the positive and negative displacement, respectively. The transition regions between the solid lines and dashed lines are the nodal lines without displacement. The common nodal point of the two lowest symmetric bending modes is located and marked with circles in Fig. 3.

## 2.3. Comparison with theoretical analyses

Blevins [13] and Leissa [14] presented the theoretical resonance frequencies and corresponding mode shapes of plate structures. Blevins [13] gave 21 combinations of boundary conditions with different width to length ratios and the frequency parameters  $\lambda$  of different modes, and estimated the resonance frequencies by

$$\omega = \sqrt{\frac{D}{\rho}} \left( \frac{\lambda}{a^2} \right), \quad (1)$$

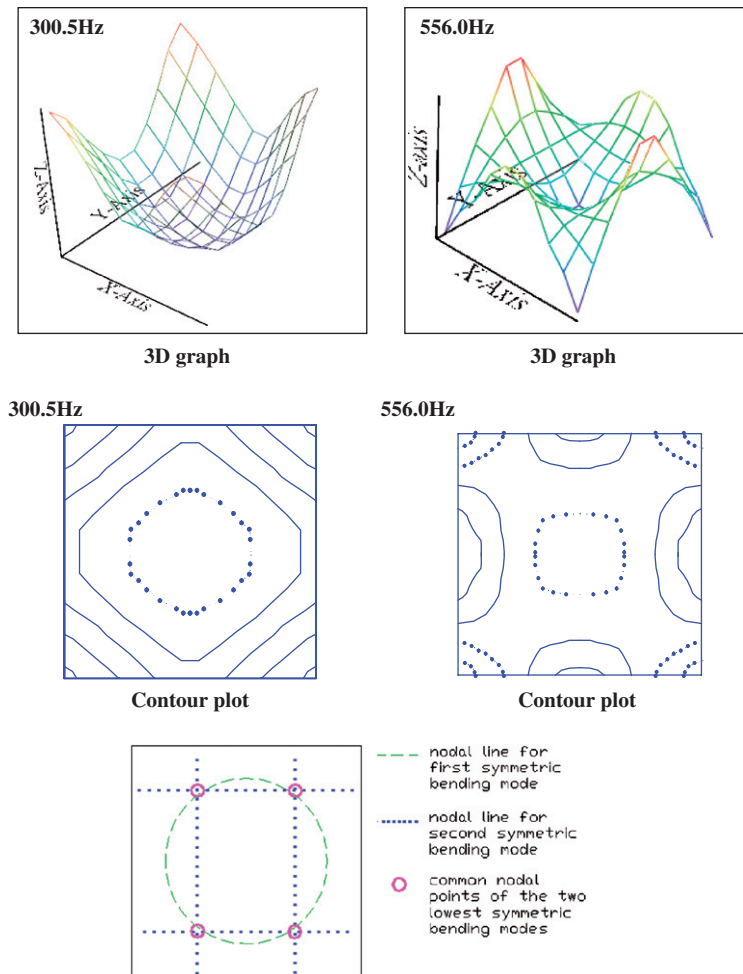


Fig. 3. The mode shapes and identified common nodal points for the lowest two symmetric bending modes of paper honeycomb panel.

where  $\omega$  is the the angular resonance frequency (rad),  $a$  is the length of the panel (m),  $\rho$  is the mass density per unit area of the panel ( $\text{kg/m}^2$ ),  $D$  is the flexural rigidity, and  $\lambda$  is the frequency parameter [13].

$$D = \frac{Eh^3}{12(1 - \nu^2)}, \tag{2}$$

where  $E$  is the Young’s modulus ( $\text{N/m}^2$ ),  $h$  is the panel thickness (m), and  $\nu$  is the Poisson’s ratio.

Based on Eqs. (1) and (2) and the frequency parameters  $\lambda$  (where the boundary condition is free along the circumference of the plate) that were provided by Blevins [13], the lowest two symmetric and the lowest four anti-symmetric bending resonance frequencies and corresponding mode shapes are given in Tables 3a and b separately. The measured mode shapes of the honeycomb panel agree well with the predicted results. The resonance frequency of the honeycomb panel and cement panel of the lowest symmetric mode resonance agrees with the predicted results with errors less than 10% (Table 3a). Furthermore, it should be noted that the center point is the common nodal point of the anti-symmetric modes (Table 3b).

### 3. Theoretical analysis of the effect of isolator position on transmissibility

The degradation of transmissibility that is attributed to the bending resonance has been predicted in Refs. [4,15] predicted values of transmissibility can be obtained from Eq. (3) in Beranek’s study [16]. The mobility of

Table 3a

The lowest two theoretical and experimental resonance frequencies of symmetric bending mode shapes for square honeycomb panel and cement panel

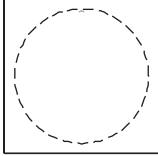
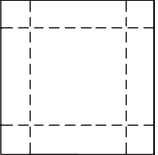
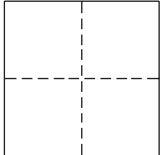
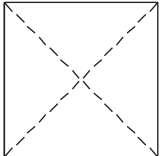
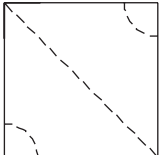
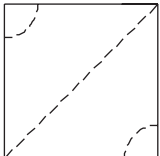
| Sequence of symmetric mode | Mode shape  | Corresponding theoretical resonance frequencies |              | Corresponding experimental resonance frequencies |              |
|----------------------------|---|---|--------------|--|--------------|
|                            |   | Paper honeycomb panel                           | Cement panel | Paper honeycomb panel                            | Cement panel |
| 1                          |  | 273.5 Hz  | 141.9 Hz     | 300.5 Hz   | 145.5 Hz     |
| 2                          |  | 688.9 Hz  | 357.5 Hz     | 556.0 Hz   | 337.5 Hz     |

Table 3b

Prediction of the lowest four resonance frequencies of anti-symmetric bending mode shapes for square honeycomb panel and cement panel

| Sequence of anti-symmetric mode | Mode shape  | Corresponding theoretical resonance frequencies |              |
|---------------------------------|---|---|--------------|
|                                 |   | Paper honeycomb panel                           | Cement panel |
| 1                               |   | 151.0 Hz  | 78.4 Hz      |
| 2                               |  | 221.6 Hz  | 114.9 Hz     |
| 3                               |  | 392.1 Hz  | 203.5 Hz     |
| 4                               |  | 392.1 Hz  | 203.5 Hz     |

the base is assumed to be negligible compared to the mobility of the floor panel

$$\text{Tr} = \frac{V}{V_o} = \frac{|M_m|}{|M_i + M_m|}, \tag{3}$$

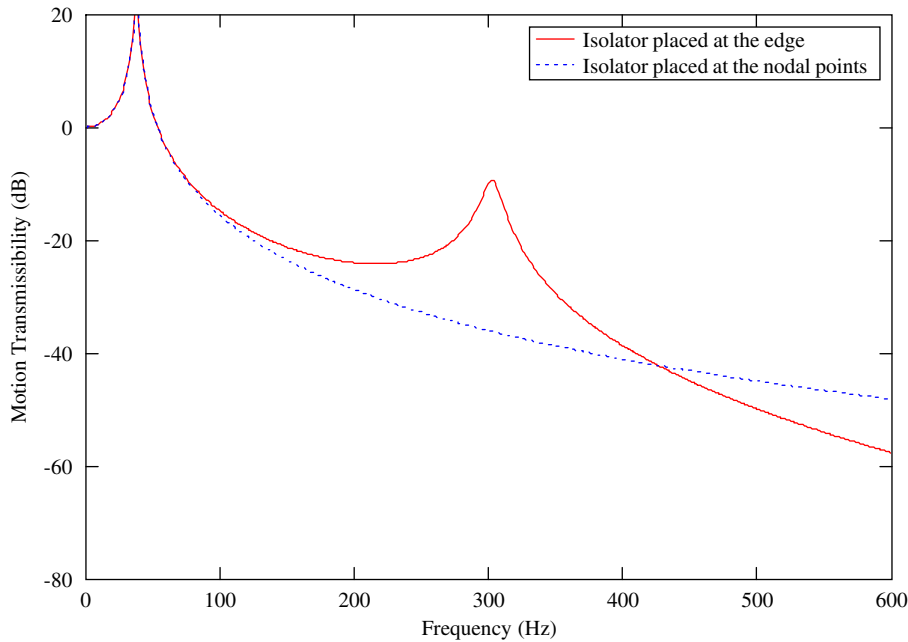


Fig. 4. Theoretical results of motion transmissibility of honeycomb panel when isolators placed at the edge and nodal points.

where  $Tr$  is the transmissibility,  $V$  is the velocity of the honeycomb floor panel,  $V_o$  is the velocity of the cement base panel,  $M_m$  is the mobility of honeycomb floor panel, and  $M_i$  is the mobility of the isolator.

Fig. 4 shows the transmissibility when the isolators are placed at the edge and the nodal points of the first bending mode when the vibration transmission path is structure borne only. When the isolators are placed at the four edges, the bending resonance peak occurs at around 300 Hz for the honeycomb panel. As the mobility depends on the bending vibration of the panel, it should be minimized when the isolators are placed at the nodal points. Thus, the peak is attenuated significantly when the isolators are placed at the nodal points of the first bending mode.

The concept of nodalization [10] may be theoretically easy to implement, but in practice several additional features must be considered. First, only a few modes of the floating floor should be controlled, which requires a small, stiff, and lightweight panel design. Second, the acoustic transmission path should be blocked effectively in the air cavity. Third, the receiver point should be at the center to avoid the effects of the anti-symmetric modes.

The following experimental tests were carried out to verify the importance of these design features.

#### 4. Test to verify the effect of isolator position in the absence of an acoustic path

##### 4.1. Experimental setup

The energy communication paths from the base to the floating floor along the structure-borne and air-borne paths are depicted in Fig. 5. It is necessary to employ experimental techniques to reduce the air-borne path to investigate the two paths separately. The experimental setup that is shown in Figs. 6a and b aims to verify the effect of isolator position on the vibration transmissibility of floating floors without an air-borne energy transmission path, which is an idealized situation. To eliminate the air-borne energy transmission path to the floor panel, four small bricks of  $100 \times 100 \times 60$  mm were arranged under the isolators to form the base structure. Impact excitation was applied to the bricks. The air-borne energy that was transmitted from the small bricks included the rigid body and bending vibration modes. The sound energy that was generated by the rigid body vibration depended on the brick surface area, which was so small that the magnitude of the

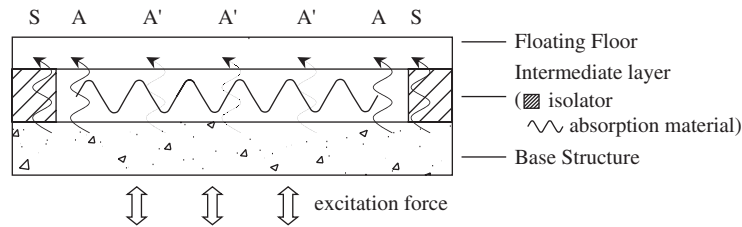


Fig. 5. Energy transmission paths of typical floating floor structure from the base structure to the floating floor via the intermediate layer. The paths marked with S are structure-borne energy transmission path via isolator; the paths marked A are air-borne energy transmission path via air gaps; the paths marked A' are air-borne energy transmission path with energy attenuation device of absorption material.

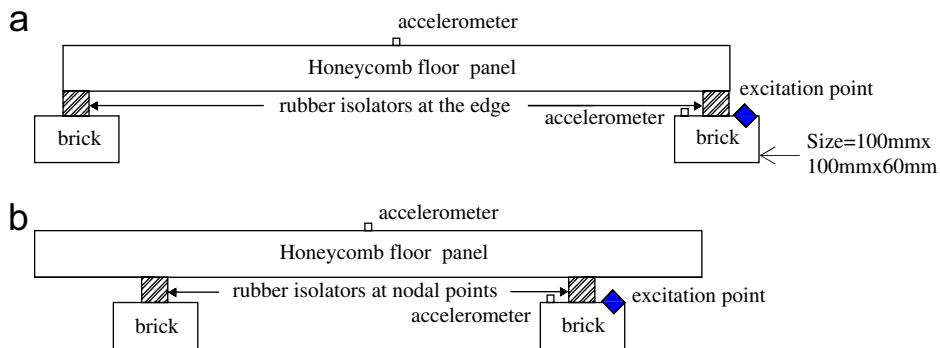


Fig. 6. Experimental setup for the motion transmissibility measurement with structure-borne energy transmission path only: (a) isolators placed at the edge; (b) isolators placed at the identified common nodal points of the lowest two symmetric bending modes.

sound that came from the rigid body vibration could be neglected. The sound energy that was generated by the bending modes of the brick could also be neglected in this measurement, as the length of each brick was only 100 mm, which meant that the first bending mode frequency was above 1 kHz. (i.e. The energy transmission from the base structure to the floor panel along the air-borne energy transmission path can be neglected.) Rubber isolators were placed on the bricks (each of which was  $30 \times 30 \times 30$  mm with a stiffness of 6847 N/m) to support the honeycomb floor panel. A steel hammer was employed to excite the structure base to generate vibration in the frequency range of 120–600 Hz. The generated acceleration on the base structure and the response acceleration on the center point of the floor panel were then measured using two accelerometers. The FRFs (acceleration on the floor panel/acceleration on the base structure), which are known as the motion transmissibility, were identified.

#### 4.2. Experimental results

The motion transmissibility when the isolators were located near the corners (Fig. 6a) and when they were placed at four common nodal points (Fig. 6b) was obtained. Figs. 7a–c show the effect of the position of the isolators on the motion transmissibility at the receiver when the transmission path was structure borne. The high coherence from 120 to 600 Hz shows that the measurement of the magnitude of the motion transmission was accurate in the test frequency range. The sudden dips below 120 Hz were probably due to a low vibration signal at the source or receiver. The phase angle of  $90^\circ$  at the two lowest symmetric bending mode resonance frequencies confirms the effects of the resonances on the motion transmissibility. When the isolators were placed at the nodal points, the vibration reduction was 10–30 dB higher in the frequency range of 120–600 Hz. These experimental results also confirm the effect of isolator position that is detailed in Fig. 3. However, in this experimental analysis, the peak at around 300 Hz was not totally eliminated, because the areas of the rubber isolators were larger than the nodal points.



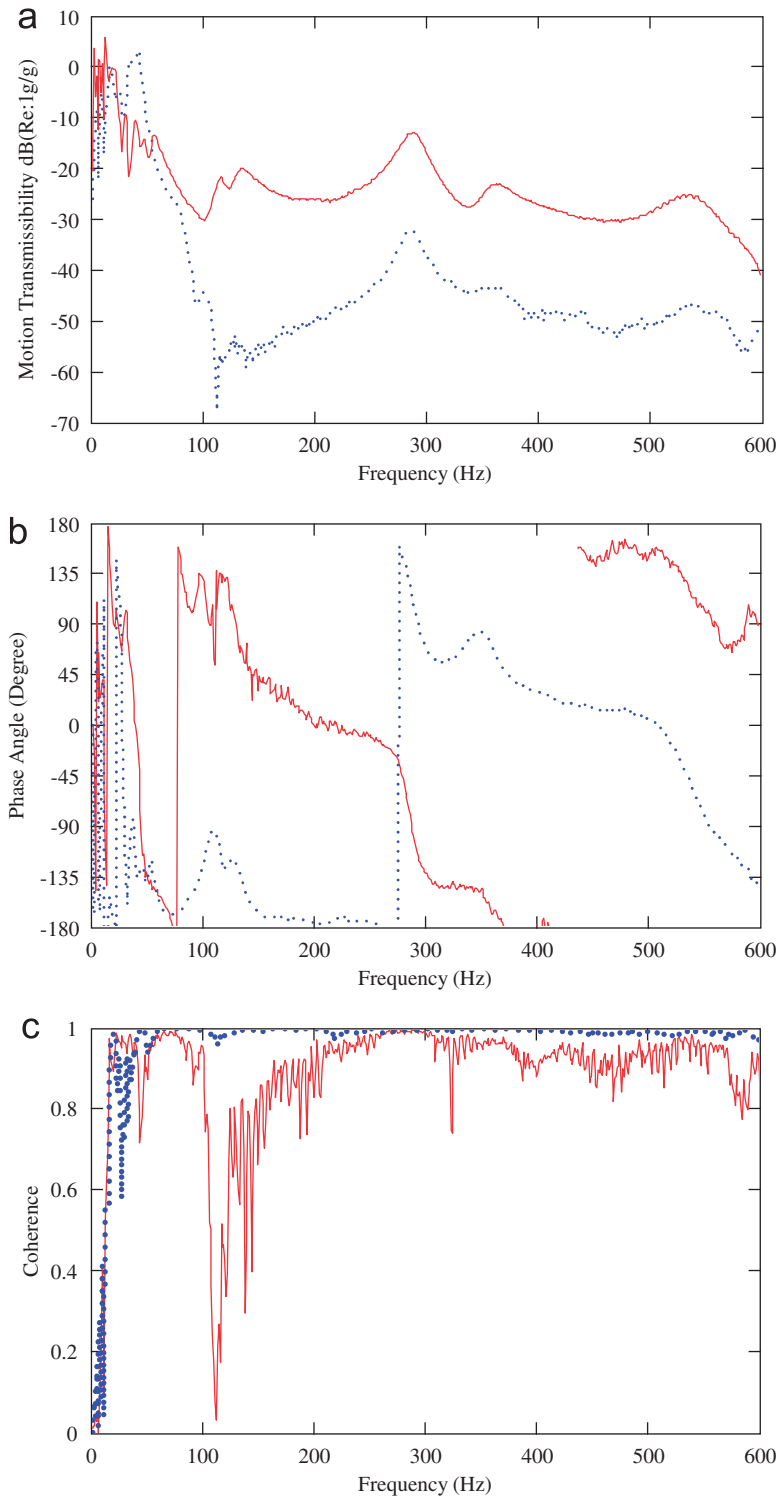


Fig. 7. Motion transmissibility results with structure-borne energy transmission path only: (a) magnitude, (b) phase, and (c) coherence. —, Sw + Awo + Ie + Amn (see Fig. 6a); - - - -, Sw + Awo + In + Amn(see Fig. 6b); Sw, Energy transmission with structure-borne path; Awo, Energy transmission without air-borne path; Ie, Four isolators place at the edge points; In, Four isolators placed at the nodal points; Amn, No acoustic insulation material used.

## 5. Test to verify the effect of an air-borne energy transmission path on a cement base structure

### 5.1. Experimental setup

In the following experiments, the cement panel used in the shaker test was selected as the structure base. The panel was a lightweight floor structure of the type that is commonly used in buildings with steel or wood frames. The honeycomb panel used in shaker test was applied as the floating floor. To prevent the overlap of the nodal points of the cement and honeycomb panels, the cement base panel was designed to be larger than the honeycomb panel.

The experimental setup that is shown in Figs. 8a and b aims to verify the effect of an air-borne energy transmission path on the vibration transmissibility of the floating floor. To eliminate the structure-borne energy transmission path, the honeycomb panel was robustly suspended above the cement panel at a height of 100 mm, as shown in Fig. 8a. A steel hammer was used to excite the cement panel to generate an air-borne sound that was then transmitted to the honeycomb panel. A microphone was placed between the two panels to detect the energy transmission from the base structure to the honeycomb panel through the air cavity. The vibration response of the honeycomb panel to the acoustic pressure was then measured.

The experimental setup in Fig. 8b includes both air-borne and structure-borne energy transmission paths. Four wooden blocks (each of which was  $70 \times 70 \times 70$  mm) were employed to support the rubber isolators to maintain a typical cavity depth of 100 mm between the floor and base panels. The wooden blocks were designed to support the rubber isolators at both the edge and nodal positions. This ensured that the vibration energy transmission from the cement panel via the wooden blocks to the honeycomb floor panel was constant for different isolator positions in the following sections.

Two strips of soft rubber were used to support the cement base panel to avoid any change in the resonance frequencies of the base panel. The boundary condition of both the honeycomb floor and the cement base panel were free at the circumference.

The shaker test in Section 2 could not be applied in the experimental test for two reasons. First, the cement base panel would have had to be tightly fixed to the vibrating head of the shaker to avoid static instability when the floor panel was placed on the cement panel, which would have affected the bending vibration resonances of the cement panel. Second, to avoid fixing the cement panel on the shaker, a large rigid panel would have had to be placed on the vibrating head of the shaker to support the test panels, which would have made the static weight of the large rigid panel too heavy for the shaker. Thus, an impact test was used instead of a shaker test.

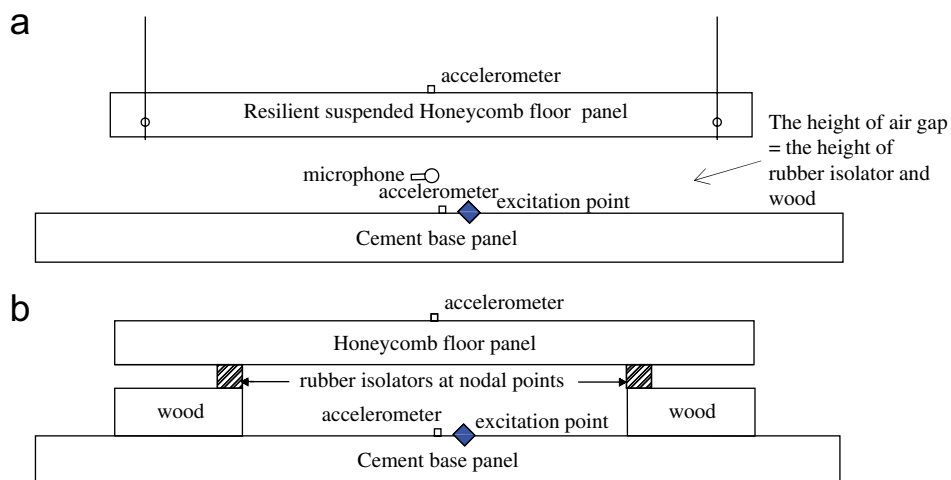


Fig. 8. Experimental setup for the motion transmissibility measurement for air-borne energy transmission path investigation: (a) air-borne energy transmission path only; (b) isolators placed at the identified common nodal points of the lowest two symmetric bending modes with both air-borne and structure-borne energy transmission paths.

## 5.2. Experimental results

The motion transmissibility of the cases in which no isolator was used and the honeycomb panel was suspended above the cement base structure (Fig. 8a) and when the isolators were placed at four nodal points between the honeycomb and cement panels (Fig. 8b) was studied.

The coherence values of the vibration (on the base panel) induced response (on the floor panel) are shown in Fig. 9c, and those of the acoustic (between the two panels) induced response (on the floor panel) are shown in Fig. 10c. In general, the coherence values are high (above 0.7) in the frequency range of 120–600 Hz. The sudden dips at certain frequencies imply that the motion transmissibility results are less accurate at these frequencies. Furthermore, a phase angle of  $90^\circ$  can be observed in the resonance frequencies (Figs. 9b and 10b), which proves that the vibration resonances were due to the acoustic pressure. The magnitude of motion transmissibility in the two cases is similar at the first and second bending modes, as shown in Fig. 9a. Hence, the test confirms that to enhance the vibration isolation performance at the receiver, both the structure-borne and air-borne energy transmission paths should be effectively isolated. This finding agrees well with the suggestion that the air that is trapped between the structure base and the floating floor plays an important role in the vibration isolation performance of floating floors [5].

In theory, the larger the air cavity the lower the air stiffness under the panel and the better the vibration isolation performance [17]. However, in practice, the air gap should not be too large because of the standing wave resonance and limited space. As the typical air cavity between the structure base and floor panel is around 100 mm, acoustic insulation material could be installed in the cavity to absorb the energy transmission.

## 6. Test to verify the effect of isolator position with a cement base structure and acoustic insulation

### 6.1. Experimental setup

The foregoing experimental results demonstrate that it is practical to use a honeycomb panel as a floating floor to improve the vibration isolation performance of lightweight cement base panels. The experimental setup in Figs. 11a and b aims to verify the effectiveness of the improvement in vibration isolation that is achieved by the installation of a honeycomb floor panel with a nodal point isolator design.

The experimental setup in this section is similar to the setup in Fig. 8b, except that insulation materials of air-borne paths have been added. The acoustic path was insulated using a vinyl sheet to cover the porous foam material, as shown in Figs. 11a and b. Vinyl sheeting is a flexible and highly damped material that is widely used in acoustic isolation in lightweight floor panels.

### 6.2. Experimental results

The motion transmissibility when the isolators were placed at the identified nodal points (Fig. 11a) and when they were placed at the edge (Fig. 11b) was studied. A sound insulation device was installed in both cases. As shown in Fig. 12a, there was a 20–30 dB vibration reduction in the frequency range of 120–600 Hz. This was due to the reduction in both the structure-borne and air-borne energy communication paths through the placement of the isolators at the nodal points and installation of acoustic insulation material. The importance of the position of the isolators can also be observed in Fig. 12a, which shows a significant vibration reduction of between 5 and 30 dB in the range of 120–550 Hz when the isolators were placed at the nodal points.

The vibration spectrum of the cement and honeycomb panels is shown in Figs. 12b and c, respectively, for the edge and nodal point isolator positions. It is noted that there is a significant peak at 145.5 Hz for the cement panel that is reduced in the honeycomb panel in both cases. Fig. 12b confirms that the bending resonance of the honeycomb panel at 300 Hz degraded the vibration isolation performance of the base panel when the isolators were placed at the edge. However, when the isolators were placed at the nodal points of the honeycomb floor panel, the vibration magnitude of the bending resonance at 300 Hz was considerably reduced (see Fig. 12c).

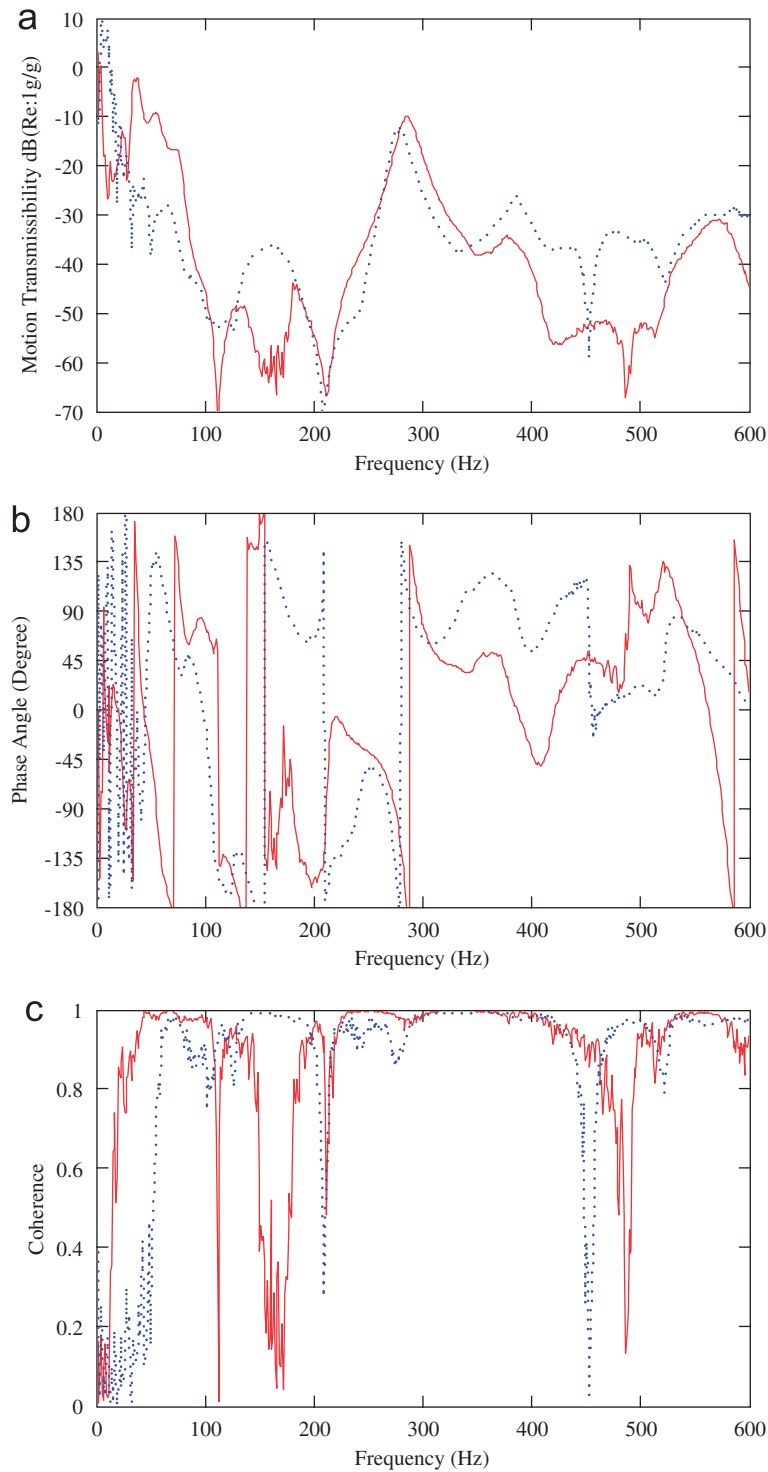


Fig. 9. Motion transmissibility results for the air-borne energy transmission path investigation: (a) magnitude, (b) phase, and (c) coherence. - - - - - , Sw + Aw + Ino + Amn (see Fig. 8a); — , Sw + Aw + In + Amn (see Fig. 8b); Sw, Energy transmission with structure-borne path; Swo, Energy transmission without structure-borne path; Aw, Energy transmission with air-borne path; Ino, No isolator used; In, Four isolators placed at the nodal points; Amn, No acoustic insulation material used.

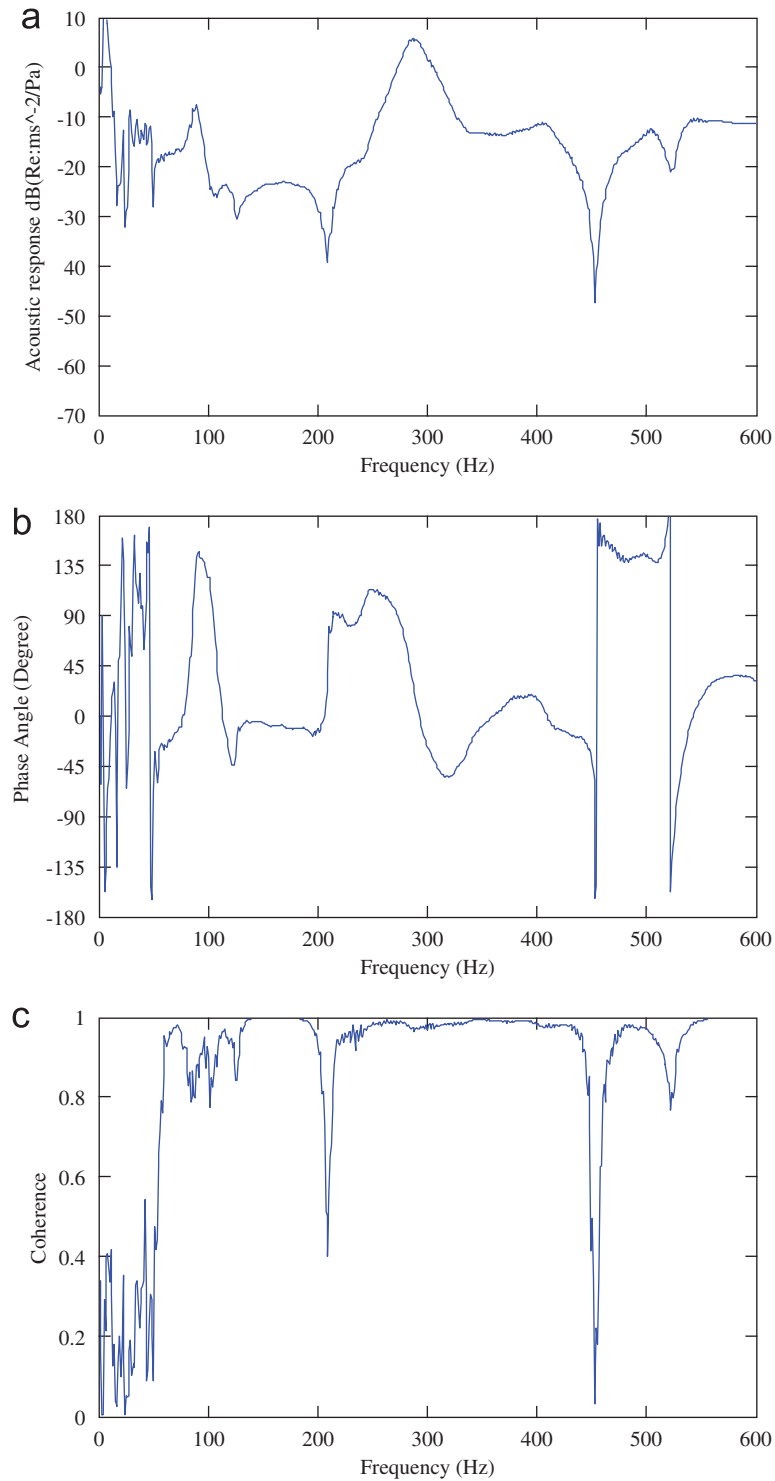


Fig. 10. Acoustic induced response results for the air-borne energy transmission path: (a) magnitude, (b) phase, and (c) coherence. — Swo + Aw + Ino + Amn (see Fig. 8a); Swo, Energy transmission without structure-borne path; Aw, Energy transmission with air-borne path; Ino, No isolator used; Amn, No acoustic insulation material used.

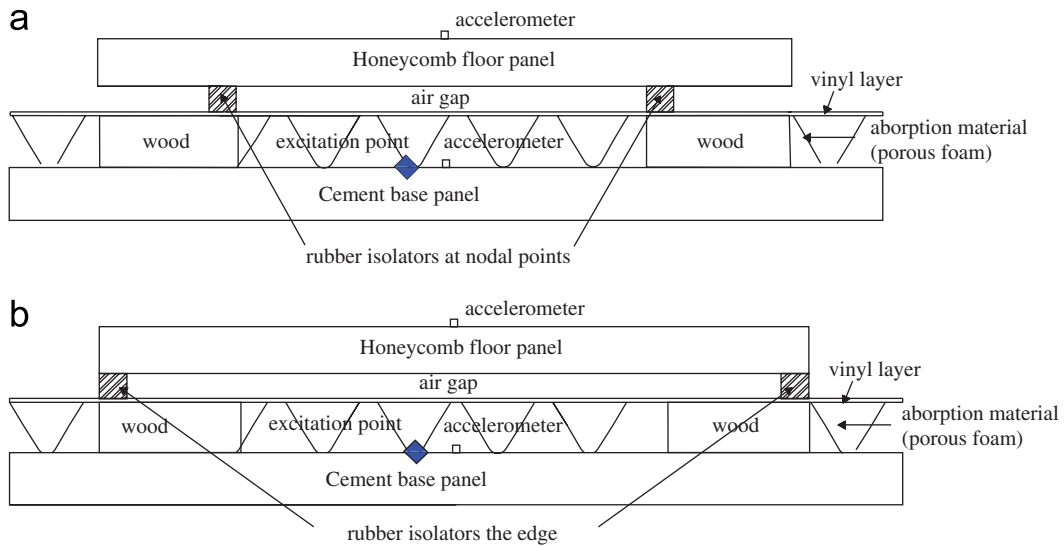


Fig. 11. Experimental setup for the motion transmissibility measurement for the conventional and new floating floor design investigation: (a) isolators were placed at identified nodal points and with sound insulation; (b) isolators placed at the edge and with sound insulation.

These findings are consistent with the theoretical analysis in Section 3, which reports that the peak vibration of a floor panel can be reduced by placing the isolators at the nodal points of the bending resonance. The summary of the experimental targets, findings and reasons from Sections 2–6 are listed in Table 4.

## 7. Comparison with conventional floating floor designs

In Fig. 13, the motion transmissibility of the proposed new floating floor installation design that is shown in Fig. 12a (dashed line) is compared with that of the conventional designs of a lightweight aluminum sandwich floating floor [9] and a cement floating floor [12] at a range of 100–800 Hz in a one-third octave band. The honeycomb floor panel of the proposed design achieves a much better vibration reduction. The poorer vibration isolation performance of the aluminum panel and cement floor is likely to be due to the isolator positions and lower bending resonances, as the floor panels in these conventional designs are larger. Furthermore, the cement floating floor is difficult to use in practice due to its heavy static loading at the base.

## 8. Potential application of the new floating floor design

In the experimental analysis in this paper, the acceleration at the center point, which is the location of the common nodal point in the anti-symmetric bending modes (see Table 3), is considered. This means that the vibration reduction performance may be even lower at other points, as the anti-symmetric bending modes of the panel may be excited. To reduce the effect of these anti-symmetric modes, the receiver should be placed at the common nodal point (center point) in these modes. Another problem is that the placement of the isolators at the identified nodal points may cause overturning when a load is added to the edge of the panel. There are two methods to tackle this problem to maintain the improved vibration isolation performance. The first is to use a table with legs that are placed at the center points of the proposed floating panel new design, as shown in Fig. 14. The device that is to be protected from vibration can then be placed on the table. The second method is to add an additional panel to the original floating floor panel, with additional isolators that are placed at the center point of the lower panel (see Fig. 15). This would reduce both the symmetric and anti-symmetric vibration resonances. This is a two-stage isolation system and is similar to the floating raft technique that is used to reduce vibration and reduce damage to equipment on ships. The arrangement of alternate isolators in the floating raft system has been theoretically found [18] (see Fig. 16) to achieve a higher level of vibration isolation, but the effect when the isolators are placed at the nodal points has not been investigated. The new

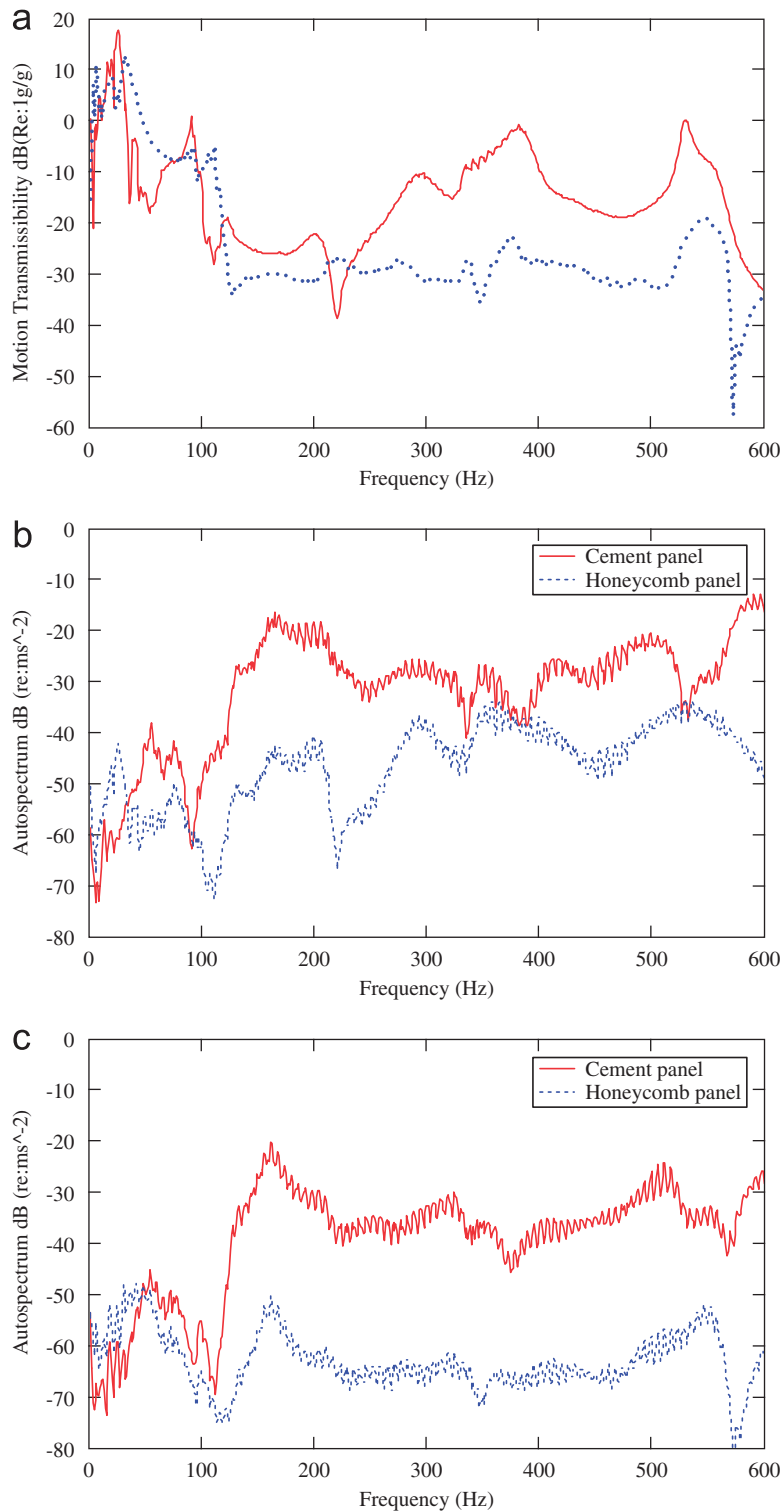


Fig. 12. (a) Comparison of vibration isolation performance with the conventional and new floating floor design; ---- $-S_w + A_w + I_n + A_m$  (see Fig. 11a) ——— $-S_w + A_w + I_e + A_m$  (see Fig. 11b);  $S_w$ , Energy transmission with structure-borne path,  $A_w$ , Energy transmission with air-borne path;  $I_n$ , Four isolators placed at the nodal points;  $I_e$ , Four isolators placed at the edge points;  $A_m$ , Acoustic insulation material used. (b) autospectrum of vibration on cement base and honeycomb floor panel when the isolator placed at the edge of the honeycomb panel (see Fig. 11b); and (c) autospectrum of vibration on cement base and honeycomb floor panel when the isolator placed at the nodal points of the honeycomb floor panel (see Fig. 11a).

Table 4  
Summary of experiments

|                       | Target  | Excitation method   | Findings  | Reasons   |
|-----------------------|---|---|---|---|
| Expt.1<br>(Section 2) | Identify the dynamic properties of the cement and honeycomb panel                   | Shaker at the center point of the panel supported with soft rubber (see Fig. 1) | The light weight honeycomb panel is a good selection for improving the vibration isolation performance of the typical light weight cement floor panel   | Resonance at 145.5 Hz of cement panel may be reduced by anti-resonance at around 140 Hz of the honeycomb panel<br><br>The bending mode at round 300 Hz of honeycomb panel should be controlled by isolators placed at the nodal points of symmetric mode (see Fig. 2) |
| Expt.2<br>(Section 4) | Verify the effects of isolator positions to transmissibility in idealized situation | Repeated impact on a small brick with steel hammer (see Fig. 6)                 | Isolator placed at the nodal point of the symmetric bending mode of floor panel is an effective vibration isolation procedure in the idealized situation with structure-borne path              | The transmissibility of isolators placed at the nodal points of symmetric mode is much lower than that of the isolators placed at the edge (see Fig. 7)   |
| Expt.3<br>(Section 5) | Verify the importance of air-borne energy transmission path                         | Repeated impact on the cement base panel with steel hammer (see Fig. 8)         | The air-borne energy transmission path for floating floor is very important   | The magnitudes of transmissibility are similar for cases with and without structure-borne path (see Fig. 9a)  |
| Expt.4<br>(Section 6) | Verify the importance of isolator position in realistic situation                   | Repeated impact on the cement base panel with steel hammer (see Fig. 11)        | Isolator placed at the nodal points of honeycomb panel is an effective method to enhance the vibration isolation performance for the typical light weight cement panel in a practical situation | The magnitudes of transmissibility can be reduced significantly when the isolators placed at the nodal when air-borne path is blocked (see Fig. 12a)  |

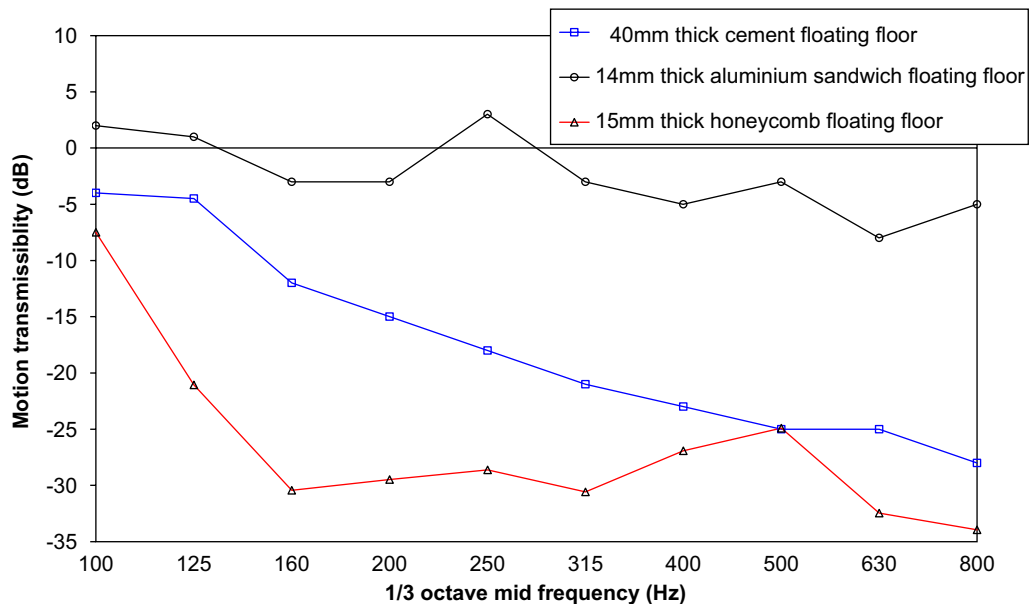


Fig. 13. Comparison of the vibration isolation performance with typical floating floor design.



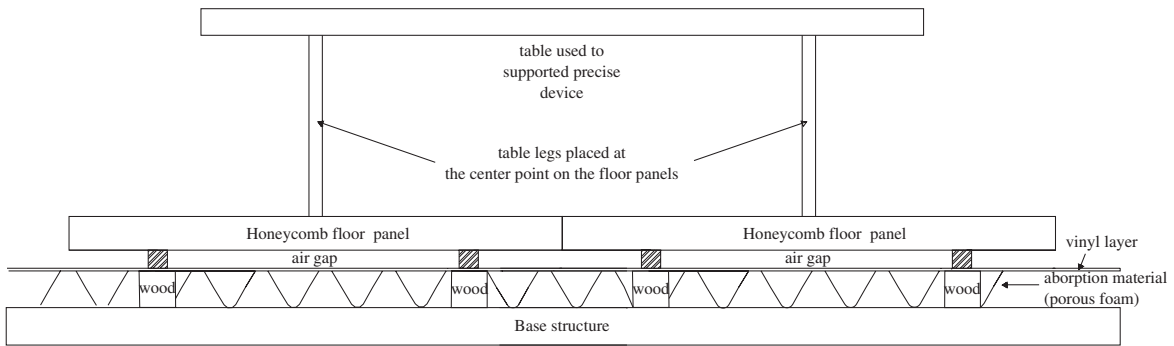


Fig. 14. A special method to reduce the anti-symmetric bending resonances and overturn problem with the new proposed floating floor design.

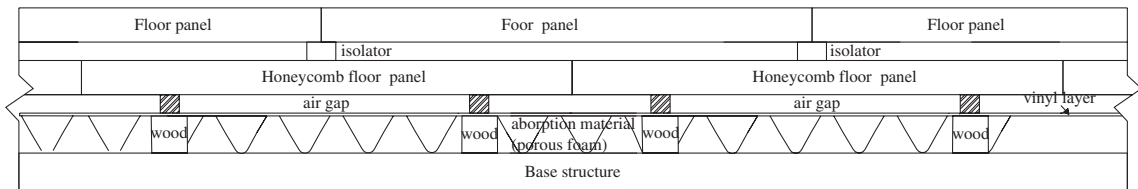


Fig. 15. A general method to reduce the anti-symmetric bending resonances and overturn problem with new proposed floating floor design.

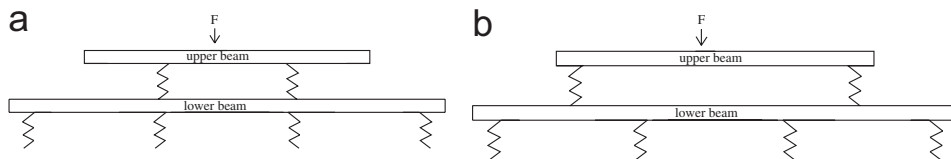


Fig. 16. Vibration reduction devices: (a) isolators placed with in-line arrangement and (b) isolators placed with alternate arrangement. Adopted from Ref. [18].

design in Fig. 15 is similar to the alternate design in Fig. 16b in that the symmetric and anti-symmetric bending modes are not excited.

## 9. Conclusion

Extensive experiments have been conducted to examine the effects of structure-borne and air-borne vibration transmission paths and confirm that an improved vibration isolation performance is achieved by the proposed new floating floor design. The results also confirm that the vibration isolation performance of a typical lightweight cement floor panel can be improved by pairing it with a honeycomb floor panel.

In general, to achieve the optimum vibration isolation performance, the following design features should be selected. First, a small ( $415 \times 415$  mm) floor panel with a high stiffness to mass ratio is recommended to increase the bending resonance frequencies of the system. Second, the isolators should be placed at the common nodal point of the lowest two symmetric bending modes of the floor panel. Third, lightweight and highly damped acoustic insulation material should be installed, together with acoustic absorption material, in the air cavity. Fourth, the receiver point should be located at the center point of the honeycomb panel so that the anti-symmetric bending modes and overturning problem can be eliminated.

The new floating floor design achieved a vibration reduction of 20–30 dB in the frequency range of 120–600 Hz. In addition, the proposed floor was found to have a 20 dB lower vibration level at the first bending resonance frequency than the conventional design in which the isolators are placed at the edges.

### Acknowledgment

The authors like to acknowledge the support of the University Grant Committee (UGC) for the project No. POLYU 5281/04E.

### References

- [1] M.D. Clark, H.L. Harry, A systematic approach used to design floor panel isolation for a commercial aircraft, *Internoise* (1996) 455–460.
- [2] A. Nilsson, Some acoustical properties of floating-floor constructions, *JASA. Journal of the Acoustical Society of America* 61 (6) (1977) 1533–1539.
- [3] M. Wollström, *Floating Floors, Models and Simulations of Vibration Characteristics*, Stockholm, 2000.
- [4] T. Kawaharazuka, T. Hiramatsu, H. Ohkawa, M. Koyasu, Experimental study on vibration reduction by isolated railway, *Internoise* (1996) 1549–1552.
- [5] C.M. Harris, *Noise Control in Buildings: A Guide for Architects and Engineers*, McGraw-Hill, New York, 1994.
- [6] C.W. Huang, C.F. Ng, Sound insulation improvement using honeycomb sandwich panels, *Applied Acoustics* 53 (1–3) (1998) 163–177.
- [7] P.R. Cunningham, R.G. White, G.S. Aglietti, The effects of various design parameters on the free vibration of doubly curved composite sandwich panels, *Journal of Sound and Vibration* 230 (3) (2000) 617–648.
- [8] H. Jutulstad, *Flytende gulv på fjaerer—lydreduserende konstruksjon for fartoy*, Institutet for Husbyggnadsteknik, Universitet I Trondheim” Norges Tekniske Hogskole, Norway, 1985.
- [9] N. Baron, Some Acoustical Properties of Floating Floors Used in Trains, Thesis, KTH Aeronautical and Vehicle Engineering, 2004.
- [10] D.J. Mead, *Passive Vibration Control*, Wiley, Chichester, New York, 1998.
- [11] X.L. Yan, Y. Xie, The effect of arrangement of isolators in coupled vibration, *Chinese Journal of Electronics Machinery Engineering* 82 (6) (1999).
- [12] L.L. Beranek, *Noise and Vibration Control*, Institute of Noise Control Engineering, Washington, DC, 1998.
- [13] R.D. Blevins, *Formulas for Natural Frequency and Mode Shape*, Yan Nostrand Reinhold Company, New York, 1979.
- [14] A.W. Leissa, *Vibration of Plates*, Acoustical Society of America through the American Institute of Physics, 1993.
- [15] C.K. Hui, C.F. Ng, The control of vibration from rail viaduct at source and receiver, *Proceedings of the 9th Western Pacific Acoustics Conference*, 2006.
- [16] L.L. Beranek, *Noise and Vibration Control*, rev ed., Institute of Noise Control Engineering, Washington, DC, 1988.
- [17] Y.Y. Lee, Structural–acoustic coupling effect on the nonlinear natural frequency of a rectangular box with one flexible plate, *Applied Acoustics* 63 (11) (2002) 1157–1175.
- [18] K. Du, X.J. Wu, G.L. Cheng, S.J. Zhu, Research of best isolation-fixing scheme of floating raft system, *Chinese Academic Journal of Naval University of Engineering* 17 (2) (2005) 92–94, 99.